

Structural, optical and morphological characterization of Sb₂S₃ thin films grown by Physical Vapor Deposition.

1st David Santos Cuz
*Departamento de Ingenieria
Electrica-SEES.
Centro de Investigacion y
Estudios Avanzados del Intituto
Politecnico Nacional, Cinvestav-
IPN, SEES*
14740, Ciudad de Mexico.,
07000, Mexico
dsantos@cinvestav.mx

2nd María de la Luz Olvera
Amador.
Departamento de Ingenieria

*Electrica-SEES.
Centro de Investigacion y
Estudios Avanzados del Intituto
Politecnico Nacional, Cinvestav-
IPN, SEES*
Apartado Postal 14740, Ciudad
de Mexico., 07000, Mexico
molvera@cinvestav.mx

3rd Sayda Dinorah Coria
Quiñones
*Unidad Querétaro.
Centro de Investigacion y
Estudios Avanzados del Intituto*

*Politecnico Nacional, Cinvestav-
IPN*
Mexico, Libramiento
Norponiente No. 2000, Fracc.
Real de Juriquilla, Querétaro,
Qro. 76230.
sayda.coria@cinvestav.mx

4th Francisco Javier de Moure
Flores.
*Facultad de Quimica.
Universidad Autonoma de
Queretaro*

Ciudad de Mexico, 76010
Santiago de Queretaro, Qro
fcomoure@hotmail.com

5th Jose Santos Cruz
*Facultad de Quimica.
Universidad Autonoma de
Queretaro*
Ciudad de Mexico, 76010
Santiago de Queretaro, Qro.
jsantos@uaq.edu.mx

Abstract—Antimony sulfide (III) (Sb₂S₃) thin films were deposited onto Corning glass substrates via physical vapor deposition technique (PVD). Commercial antimony sulfide powder was used as evaporation source and it was annealed at three different temperatures 250, 275 y 300 °C in an inert atmosphere of Argon (Ar). The structural, optical, and morphological properties of annealed Sb₂S₃ thin films were analyzed in order to be applied as absorbent layer in thin-film solar cells. All films presented an orthorhombic phase of Sb₂S₃, crystal size between 21-25 nm, transmittance values in the UV-Vis region oscillating in the 20-80% range, and a bandgap around 1.7 eV.

Keywords—Antimony Sulfide, metal chalcogenides, PVD, Thermal annealing.

I. INTRODUCTION

The stibnite or Antimony Sulfide (Sb₂S₃) is present as raw material in the earth's crust. Sb₂S₃ present an orthorhombic structure, semiconducting properties in pure form with a p-type conductivity, and very attractive optical properties for solar cells applications, since it has an optical absorption coefficient value (α) greater than $1.5 \times 10^5 \text{ cm}^{-1}$ and direct energy bands with a bandgap value between 1.4 to 2.2 eV. Antimony Sulfide (III) has been deposited in thin film form by different techniques, such as chemical bath deposition (CBD), physical vapor deposition (PVD), spin-coating, and pulsed laser deposition (PLD), among others, being the most used and reported the

PVD and CBD techniques. In general, irrespective of the deposition technique used, the Sb₂S₃ presents an amorphous structure, therefore an annealing treatment is necessary to obtain a well-defined orthorhombic structure. The application field of the metal chalcogenides in thin film form is broad, for example, in memory devices, electronics flexible, thin film photovoltaic devices, and light detectors, etc. According to the literature, as was stated above, the PVD is one of the most widely used deposition techniques for processing Sb₂S₃ thin films, this fact is due to the PVD technique provides a clean environment with well controlled deposition conditions that leads to obtain uniform, high purity, and free of defects materials. [1-10, 17-22]

In this work we are reporting partial results on evaporated Sb₂S₃ films, seeking to obtain materials with adequate characteristics for future application as an absorbent layer in thin film solar cells whose window layer would be CdS. The effect of the magnitude of the annealing temperature on the structural, optical, and morphological characteristics as compared with those not thermally treated films is presented.

II. EXPERIMENTAL PROCEDURE

A. Films deposition by PVD

The Sb₂S₃ films were deposited onto Corning glass substrates by the physical vapor deposition, PVD, technique in an Oerlikon Balzers model 350 VAC evaporator, using a powder

of Sb_2S_3 (99.999%, from Sigma Aldrich) as precursor. The electrical current of the evaporation system was varied between 80-220 A, in intervals of 20 A, resulting an optimum current of 200 A, whereas the substrate-source distance was optimized at 16 cm, since at this a homogeneous deposit was achieved on the entire substrate. The camera pressure was kept constant at 10^{-4} mBar. Subsequently to the films deposition, thermal treatments at three different temperatures, 250, 275, and 300 °C in an inert atmosphere of argon (EA), during 30 min, were carried out. Higher annealing temperatures than 300 °C were also tested, but the deposited Sb_2S_3 films presented lot of surface defects, such as pin-holes, high roughness, poor covering or porosity observed by naked-eye, this despite of testing reduced treatment time at 5 min, the above is possibly due to it's low sulfur vapor pressure and, low melting temperature (115 °C).

B. Films characterization

Thicknesses of deposited Sb_2S_3 films were measured by mechanic profilometry using a KLA Tencor model D-100 equipment. The X-ray diffraction, XRD, patterns were obtained with a PaNalitical Xpert Pro diffractometer using the $\text{CuK}\alpha$ ($\lambda=1.54178$ Å) emission and a scanning range from 10 to 60°. The surface morphology and composition of the samples were analyzed by Scanning Electron Microscopy, SEM, and EDS techniques on a JSM-7401F JEOL microscope with an energy of 2 KeV and 50000X. The optical characterization consisted in obtaining the UV-Visible spectra in the 300-1050 nm range using a Thermo-Scientific, model S10, spectrophotometer. From these optical transmission spectra the energy bandgap values were calculated by the Tauc method, which consists of extrapolating the linear region to the horizontal axis, $(\alpha h\nu)^2=0$, in a $(\alpha h\nu)^2$ vs energy ($h\nu$) plot. The excellent linear fit obtained for all the samples confirmed the bands type as direct.

III. RESULTS AND DISCUSSION

In order to analyze the influence of the thermal treatment and its magnitude temperature on the physical properties of the Sb_2S_3 films, the same characterization was made in both as-grown and thermal treated films. Samples were identified with the annealing temperature value, SbS-E-As-grown, SbS-EA-250, SbS-EA-275, and SbS-EA-300.

A. Films thickness

Figure 1 depicts the variation of the thickness as a function of the annealing temperature. The as-grown sample shows a higher thickness value (207 nm) than all the thermal treated samples. However, when samples are annealed at 250 °C during 30 min, the thickness decreases abruptly, but as the annealing temperature is increased the thickness values also increment.[26] This effect could be associated with a reordering or compaction of the films structure.

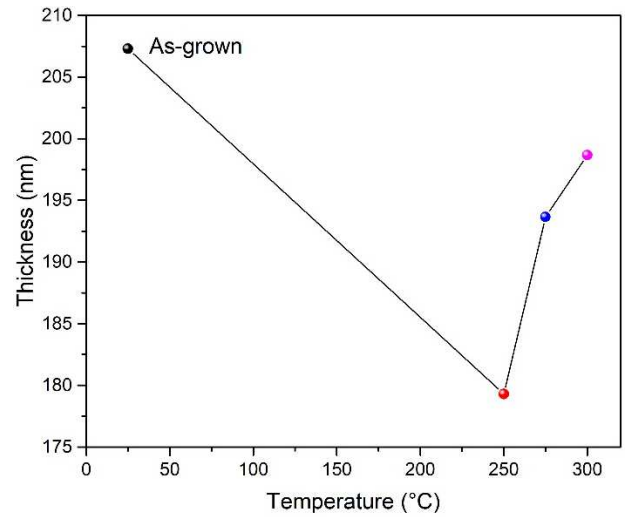


Figure 1. Thickness films as a function of the three annealing temperatures used, 250, 275 and 300 C. Red-250 °C (179 nm), blue-275 °C (194 nm), and pink-300 °C (199 nm).

B. Structural properties

All samples were analyzed by XRD. Figure 2 shows the X-ray diffractograms. It was found that as-grown films were amorphous, irrespective of the magnitude thickness (this result is not presented in this work). However, after a heat treatment from 250 °C and higher temperatures the characteristic peaks of the orthorhombic phase appeared in all the samples, although the intensity of the peaks varied. In Table 1 are reported some structural parameters calculated from the X-ray diffractograms, crystallite size (D), microstrain ($\epsilon = b\cos(\theta)/4$), and dislocation density ($\delta = D^{-2}$).

Crystallite sizes were determined by using the Scherrer's equation, $D = 0.9 k_{\text{Cu}}/B\cos(\theta)$, where k_{Cu} is the wavelength of copper radiation (1.5406 Å), B is the full-width at half-maximum (FWHM) of the highest peak, and θ is the Bragg angle in radians, for this calculation was used the peak located around 25 ° for the value of 2θ in all the samples.

From the analysis of the results, it can be observed a variation in the grain size as a function of the magnitude of the annealing temperature. Meanwhile, the stress behavior and the density of dislocations did not present an important variation on the values, indicating that annealing treatment does not influence in a significant way. [23]

Table 1. Cristal size (D), microstrain (ϵ) and dislocation density (δ) of Sb_2S_3 films grown by PVD.

TEMPERATURE (°C)	D (nm)	ϵ ($\times 10^{-3}$)	$\delta \times 10^{15}$ (LINES/m ²)
SbS-EA-250	21	1.60	2.09
SbS-EA-275	25	1.37	1.51
SbS-EA-300	24	1.45	1.67

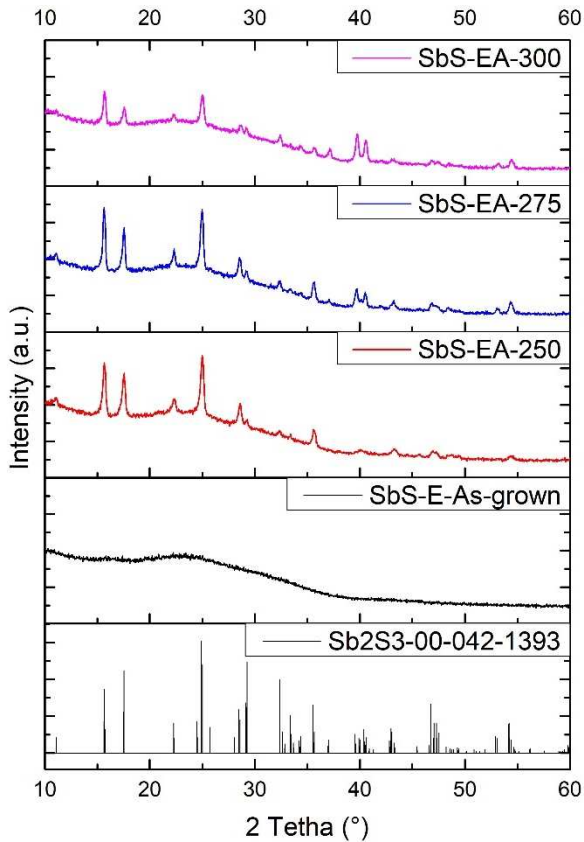


Figure 2. X-ray diffractograms of Sb_2S_3 thin films deposited by PVD at different deposition temperature. Black-as-grown, red-250 °C, blue-275 °C, and pink-300 °C.

C. Optical properties

The transmission spectra of the samples deposited by PVD before and after the annealing treatment at different temperatures are shown in Figure 3a. The optical transparency and absorption edge shown in the spectrum of the as-grown sample are clearly different from the rest, this result is evidence of the influence of the thermal treatment on the optical characteristics of the samples. The transmission spectra of all the thermal treated samples are closely similar, irrespective of the temperature, consequently, the energy bandgap values of as-grown and thermal treated samples differs in a significantly manner.

The absorption edge difference between as-grown and annealed films is indicative of the existence of different phases, and it can be appreciable in the change of color of the samples. As-grown films showed an orange color with a bandgap calculated around 2.2-2.4 eV, whereas samples with a thermal treatment presented a bright dark-brown color and bandgap values oscillating between 1,70 and 1.75 eV. These results are consistent with the structural analysis, since the material is transformed from an amorphous to an orthorhombic phase.

Figure 3b shows the bandgap values calculated from the analysis of Tauc's plots. [24, 25]

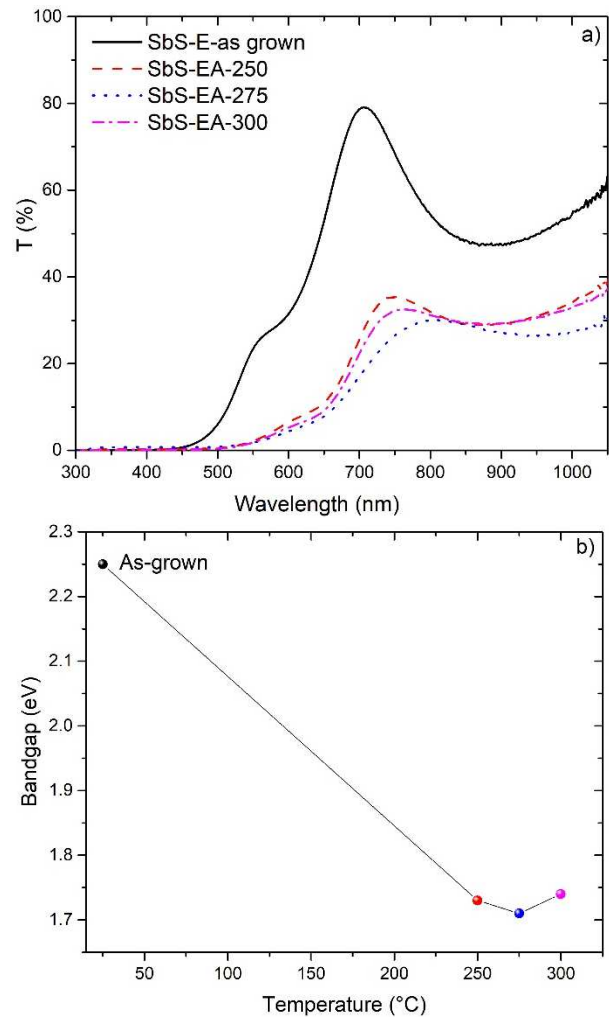


Figure 3. a) Transmittance spectra of Sb_2S_3 thin films deposited by PVD. Black-as-grown, red-250 °C, blue-275 °C, and pink-300 °C. b) Energy bandgap values as a function of the thermal treatment temperature, calculated from Tauc's plots.

D. Films composition

Figure 4 presents the Sb and S contents in every sample in atomic percentage, at %. The atomic percentage values were estimated by EDS analysis. From this graph it can be observed that, in general, the S content decreases as the temperature of the thermal treatment increases. A reverse behavior is presented with Sb, due to its low vapor pressure and high temperature this element (S) suffers a decrease in this percentage and, as a consequence when an element decreases its fraction, the percentage of remaining elements increase its fraction ratio but not its number of atoms. However, samples annealed at 250 and 275 °C present similar Sb and S concentrations. According to other results presented in the scientific literature, the expected atomic concentration to obtain an orthorhombic phase is 60 %-S, and 40 %-Sb, which was obtained under a thermal treatment performed at 300 °C. It is worth of mention that a quantitative analysis obtained from EDS is not reliable at all, and more measurement with a different technique it is

necessary in order to get reliable conclusions, for example, analysis by Secondary Ion Mass Spectrometry, SIMS.

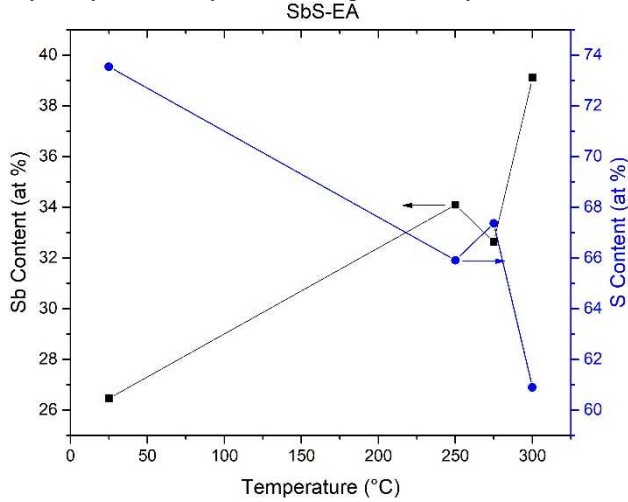


Figure 4. Concentrations of Sb and S in the Sb_2S_3 films, obtained from EDS analysis.

E. SEM analysis

SEM images are shown in Figures 5a-d. The as-grown sample (Figure 5a) present many like white round agglomerates onto a surface covered by tiny grains; after the heat treatments the size of these agglomerates increases in a significantly way, and its number decreases, this is due to the coalescence of the small ones. The biggest and most irregular agglomerates were present in samples annealed at 275 °C (Figure 5c), where the average agglomerates size was estimated around 300 nm. Sample annealed at 300 °C seems to be more uniform with lesser number of surface agglomerates; the grain boundaries are clearer, as compared with the other films, which are not visually well defined. In resume, we consider that Sb_2S_3 sample thermally treated at 300 °C present the best morphological characteristics and corresponds to its structural analysis.

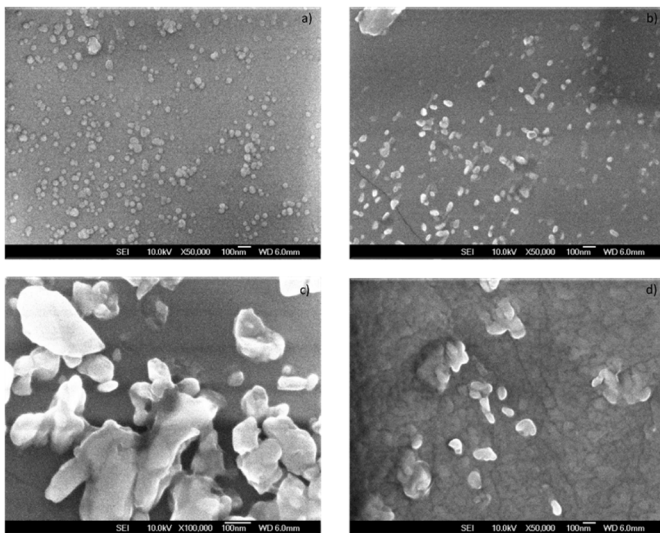


Figure 5. SEM images of a) as-grown, b) 200 °C, c) 275 °C, and d) 300 °C

IV. CONCLUSIONS

Sb_2S_3 thin films were deposited onto Corning glass substrates by PVD technique, subsequently these were thermally treated in an inert atmosphere of Argon at different temperatures. The orthorhombic structure was confirmed in all the annealed samples. The crystallite size was estimated using Scherrer's equation, obtaining values between 21 and 25 nm. A decreasing in the bandgap values, around 0.55 eV, was observed in the Sb_2S_3 samples after the annealing treatments. According to the SEM images, the best morphology was presented in sample annealed at 300 °C, since a more uniform surface with less surface agglomerates number, and well-defined grains were observed. Additionally, samples treated at 300 °C showed contents of Sb and S around 40 and 60 at %, that corresponds to the stoichiometry concentrations according to other reported results.

Finally, we consider that, the processed Sb_2S_3 thin films by PVD could be potentially applicable as absorbent layers in thin film solar cells, in combination with CdS acting as window layer. However, for this, it might be necessary the optimization of thickness films, because the diffusion length of the holes and the optical coefficient of absorption have to be considered.

ACKNOWLEDGMENTS

The authors acknowledge the technical support received from M. Guerrero, A. García-Sotelo, and Z. Rivera from Physics Department, and A. Tavira-Fuentes, M. Luna-Arias and M. Galván-Arellano from Solid State Electronics Section, both from Cinvestav-IPN.

REFERENCES

- [1]. Nair. P. K. et al, Heterojunction CdS/Sb₂S₃ solar cells using antimony sulfide thin films prepared by thermal evaporation, *Thin Solids Films* 569, pp 28-34, 2014.
- [2]. Fang G. et al, Efficient planar Sb₂S₃ solar cells using a low-temperature solution-processed tin oxide electron conductor, *Phys. Chem.* 2016.
- [3]. Mathew X. et al, Vacuum coated Sb₂S₃ thin Films: Thermal Treatment and the evolution of its physical properties, *Materials Research Bulletin* 90 pp. 285-294, 2017.
- [4]. Parize R. et al, In situ analysis of the crystallization process of Sb₂S₃ thin films by Raman scattering and X-ray diffraction, *Materials and Design* 121, pp. 1-10, 2017.
- [5]. Grozdanov I. et al, Fabrication of amorphous Sb₂S₃ films by chemical deposition, *Journal of Non-Crystalline Solids*, pp. 77-83, 1994.
- [6]. Calixto-Rodríguez M. et al, A comparative study of the physical properties of Sb₂S₃ thin films treated with N₂ AC plasma and thermal annealing in N₂, *Applied Surface Science* 256, pp. 2428-2433, 2010.
- [7]. Desai J.D. et al, Solution growth of microcrystalline Sb₂S₃ thin films from thioacetamide bath, *Journal of Non-Crystalline Solids* 181, pp. 70-76, 1995.
- [8]. Mane R. S. et al, Thickness-dependent properties of chemically deposited Sb₂S₃ thin films, *Materials Chemistry and Physics* 82, pp. 347-354, 2003.

- [9]. Lokhande C.D. et al, XRD, SEM, AFM, HRTEM, EDAX and RBS studies of chemically deposited Sb_2S_3 and Sb_2Se_3 thin films, *Applied Surface Science* 193, pp. 1-10, 2002.
- [10]. Lokhande C.D. et al, Non-aqueous chemical bath deposition of Sb_2S_3 thin films, *Thin Solids Films* 353, pp. 29-32, 1999.
- [11]. Mark Fox, *Optical Properties of Solids*, Oxford University Press, Second Edition, 2010.
- [12]. Pankove I. J, *Optical Processes in Semiconductors*, Dover Publications, Inc. New York, Chapter 4, 1971.
- [13]. Byskov-Nielsen J, Shorth-Pulse laser ablation of metals: Fundamentals and application for micro-mechanical interlocking, PhD Thesis August 2010.
- [14]. Mihai Stafe et al, *Pulsed Laser Ablation of Solids, basics, theory and applications*, Springer, 2014.
- [15]. Langford J.I. and Wilson A. J.C., Sherrer after Sixty Years: A Survey and Some New Results in the Determination of Crystallite Size, *J. appl. Cryst.*, 11, pp 102-113, 1978.
- [16]. F. de Moure-Flores, CdTe thin films grown by pulsed laser deposition using powder as target: Effect of substrate temperature, *Journal of Crystal Growth* 386, pp. 27-31, 2014.
- [17]. Arshad Hussain et al, Characterization of Cu_3SbS_3 thin films grown by thermally diffusing Cu_2S and Sb_2S_3 layers, *Surface and Coatings Technology* 319, pp 294-300, 2017.
- [18]. Y. Rodriguez-Lazcano, M. Nair, P. Nair, Photovoltaic pin structure of Sb_2S_3 and CuSbS_2 absorber films obtained via chemical bath deposition, *J. Electrochem. Soc.* 152, pp G635-G638, 2005.
- [19]. Z.S. El Mondouh, S.N. Samala, Some Physical properties of evaporated thin films of antimony trisulphide, *J. Mater Sci* 25, pp 1715-1718, 1990.
- [20]. M.S. You et al, Oxide-free Sb_2S_3 sensitized solar cells fabricated by spin and heat-treatment of $\text{Sb(III)(Thioacetamide)}_2\text{C}_{13}$, *Org. Electron. Phys. Mater Appl.* 21, pp 155-159, 2015.
- [21]. R.G. Avilez Garcia et al, Antimony sulfide (Sb_2S_3) thin films by pulse electrodeposition: effect of thermal treatment on structural, optical and electrical properties, *Mater. Sci. Semicond. Process.* 44, pp 91-100, 2016.
- [22]. J. George, M.K. Radhakrishnan, Electrical conduction in coevaporated antimony Trisulphide films, *Solid, State Commun.* 33, pp 987-989, 1980.
- [23]. Singh P., and Kumar R., Influence of high-energy ion irradiation on the structural, optical, and chemical properties of polytetrafluoroethylene, *Adv. Polym. Technol.*, Vol. 33, No. 3, pp. 21410-21418, 2014.
- [24]. Mark Fox, *Optical Properties of Solids*, Oxford University Press, Second Edition, 2010.
- [25]. Pankove I. J, *Optical Processes in Semiconductors*, Dover Publications, Inc. New York, Chapter 4, 1971.
- [26]. Wang Y. Y., Influence of post-annealing treatment on the structure properties of ZnO films, *Applied Surface Science*, 241 pp 303-308, 2005.